World Academy of Science, Engineering and Technology
International Journal of Electrical and Computer Engineering
Vol:11, No:8, 2017

Ice Load Measurements on Known Structures Using Image Processing Methods

Azam Fazelpour, Saeed R. Dehghani, Vlastimil Masek, Yuri S. Muzychka

***Abstract*—**This study employs a method based on image analyses and structure information to detect accumulated ice on known structures. The icing of marine vessels and offshore structures causes significant reductions in their efficiency and creates unsafe working conditions. Image processing methods are used to measure ice loads automatically. Most image processing methods are developed based on captured image analyses. In this method, ice loads on structures are calculated by defining structure coordinates and processing captured images. A pyramidal structure is designed with nine cylindrical bars as the known structure of experimental setup. Unsymmetrical ice accumulated on the structure in a cold room represents the actual case of experiments. Camera intrinsic and extrinsic parameters are used to define structure coordinates in the image coordinate system according to the camera location and angle. The thresholding method is applied to capture images and detect iced structures in a binary image. The ice thickness of each element is calculated by combining the information from the binary image and the structure coordinate. Averaging ice diameters from different camera views obtains ice thicknesses of structure elements. Comparison between ice load measurements using this method and the actual ice loads shows positive correlations with an acceptable range of error. The method can be applied to complex structures defining structure and camera coordinates.

***Keywords*—**Camera calibration, Ice detection, ice load measurements, image processing.

I. Introduction

STRUCTURE icing is a phenomenon influencing marine and offshore activities during cold seasons in Arctic regions [1]-[3]. Monitoring ice conditions plays an important role to apply de-icing in proper situations. Models have been established to predict the amount of ice load on marine structures [3], [4]. Ice detection and ice load measurements are challenges in marine icing research and have been investigated for years [5]-[7].

Current methods for modeling and measuring ice loads are based on physical properties, which need expensive equipment to be measured, and human interference, which causes safety hazards. Developing algorithms to predict and remove ice accumulation is automatically an essential component to reduce hazards and cost [1]. Image processing techniques have been established for ice monitoring, and are used to calculate the ice thickness on power transmission lines. The ice thickness on transmission lines is calculated applying edge detection and thresholding algorithms. Ice thicknesses are calculated by the subtraction of uniced and iced line thicknesses [8]. In another study, two cameras are employed to capture images of an iced power transmission lines. The matched corresponding points are found in the images establishing correlation methods. The edges of accumulated ice are detected using 3D coordinates obtained from two existing images [9]. The ice thickness of a cylindrical structure is measured employing a thermal camera. Thermal imaging is not affected by background color and light [10]. The combination of visual and thermal imaging is conducted to calculate the ice thickness on a structure and leads to detect the ice area more accurately than using a single type image [11]. Current image based methods can measure ice thickness on simple structures. Ice load measurements based on image processing for complicated structure can provide more advantages for ice monitoring.

In this paper, a method for ice load measurement defining the information of a known structure is developed. Using the structure information and camera position, a scheme of the structure is drawn in the image frame. An experimental setup is performed to capture images and obtain real measured data. Applying the threshold method and a morphological algorithm, the ice area is extracted from captured images. The ice load of each component of the structure is calculated and the total ice load is then obtained by the summation of component ice loads.

II. Methodology

Intersection nodes of the structure and its bar elements are defined in a determined coordinate system. This coordinate system is named the world coordinate system. The world coordinate system is converted to the camera coordinate system using extrinsic parameters, including rotation matrix, R, and translation matrix, t. These two matrices show the camera position and angle with respect to the world coordinate system. To obtain the structure coordinate in the image plane, intrinsic parameters are calculated using camera calibration. Intrinsic parameters are defined as a matrix, K, including focal length, image coordinate system origin, and correction parameters. Equation (1) shows converting a point in the world coordinate system, P_{wc}, to the image coordinate system, p_{ic}, using intrinsic and extrinsic parameters [12].

$$p_{ic} = K[R|t]P_{wc} \quad (1)$$

Using (1), each intersection node of the structure, P_i, with the coordinate of (X_i, Y_i, Z_i) in the world coordinate system is

Azam Fazelpour and Vlastimil Masek re with the Department of Electrical Engineering, Memorial University of Newfoundland, St. John's, NL, Canada (e-mail: a.fazelpour@mun.ca, masek@mun.ca).

Saeed R. Dehghani and Yuri S. Muzychka are with the Department of Mechanical Engineering, Memorial University of Newfoundland, St. John's, NL, Canada (e-mail: srdehghani@mun.ca, yurim@mun.ca).

transformed to p_i with the coordinate of (x_i, y_i) in the image coordinate system. The connections between the intersection nodes are defined in the image plane. Fig. 1 illustrates the coordinate conversion. Using this method, the structure is traced in the image plane according to the camera position and angle without capturing any image. The schemed structure is then restored in a binary format.

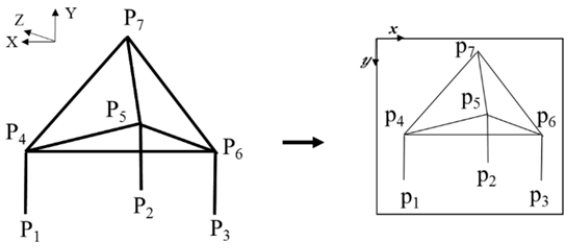

Fig. 1 Structure coordinates conversion from a 3D to a 2D coordinate system

Images are captured when ice is fully accumulated and stable. The Otsu thresholding method is used to detect the iced structure in the image [13]. The result of this method is a binary image with a value of 1 for the iced structure and a value of 0 for the background. As the block diagram in Fig. 2 illustrates, the result of ice detection is combined with the result of structure detection to calculate ice thickness for each part of the structure. Predetermination of the structure coordinates in the image, shown in Fig. 1, helps to remove irrelevant areas detected as ice in the created binary image.

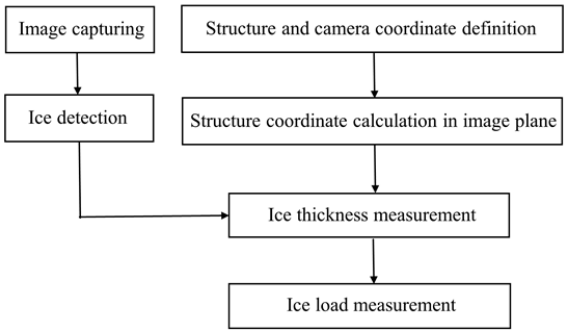

Fig. 2 Block diagram of ice load measurement

To find the ice thickness of each element independently, the data corresponding to the joints between the elements of the structure are removed in the binary image. This occurs using the joint coordinates, p_i, obtained in the image coordinate system. Fig. 3 shows the settling of ice and a selected part of the structure after removing the joints. The thickness of the element, r_i, is calculated using its detected surface area, S_i, in the binary image and its length, h_i which are shown in (2). The thickness values are calculated counting the number of ice pixels. Using camera parameters, the thickness values are obtained in the metric system [14]. Employing the calculated ice thicknesses, ice density, ρ, element length, l, and element radius, r_c, the ice load of each element, m_i, is calculated in (3). The total ice load, M, is concluded by the summation of the calculated element ice loads.

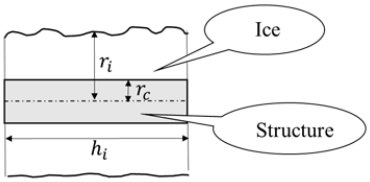

Fig. 3 Ice accumulated on the structure

$$r_i = S_i/2h_i \tag{2}$$

$$m_i = \rho\pi l_i(r_i{}^2 - r_c{}^2) \tag{3}$$

$$M = \sum m_i \tag{4}$$

This algorithm calculates the ice thickness of elements including overlaps. In the case where two elements of the iced structure are detected as a single element in the binary image, the detected ice thickness will be larger than each iced element thickness. The difference between real thicknesses and detected thicknesses is estimated by the surface area surrounded by the elements. Subtracting surface between these two elements from the measured ice surface area in the binary image is used to calculate the ice thickness of elements overlapped.

Different ice thicknesses are calculated based on camera positions and angles of view. Fig. 4 shows an elliptical cross section of a cylinder covered by ice in three different views. Locating the camera in the point view1, the ice cross section seems a circle with a diameter equal to the minor axis of the ellipse, D_1. A larger circle with a diameter of D_3 is detected if the camera is located at point view3. Setting the camera in point view2, a medium-size circle with diameter D_2 is obtained and its surface area is closer to the ellipse surface area. Calculating different ice thicknesses from different views may cause underestimation or overestimation. The average of the calculated ice thicknesses from different views provides more accurate ice thickness estimations.

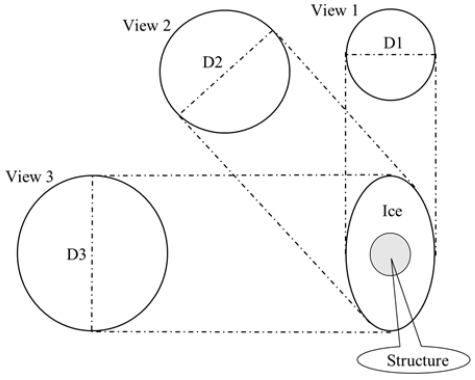

Fig. 4 The schematic of an iced structure with ellipse cross section from different views

III. Experimental Setup

A set of experiments was conducted in a cold room with a

temperature of -20 ± 1℃. Nine cylindrical elements with a diameter of 1 cm are welded to form a pyramidal structure, Fig. 5. The geometry of the complex structure is known. The length of the legs of the structure is 15 cm and the other bars lengths are 30 cm. The structure is unsymmetrically covered by saline ice with a salinity of 35‰. The ice load is measured 700 g using an accurate digital scale.

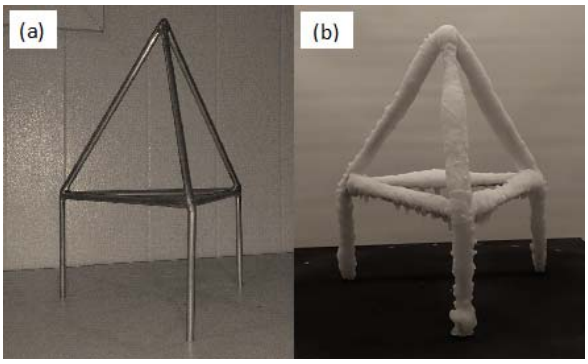

Fig. 5 The known structure used for experiments (a) The pyramidal structure with no ice, (b) The iced structure

The structure is located on a circular disk graded from 0° to 360° to provide different angles of view. The disk is able to rotate around its center in intervals of 15°. The origin point of the world coordinate system is located at the center of the disk. The structure intersection node coordinates and the connection between them are defined with respect to the world coordinate system. The camera is located at a distance of 65 cm and a height of 15 cm with respect to the center of the disk. Disk rotation provides 24 various views of the structure for camera imaging, see Fig. 6.

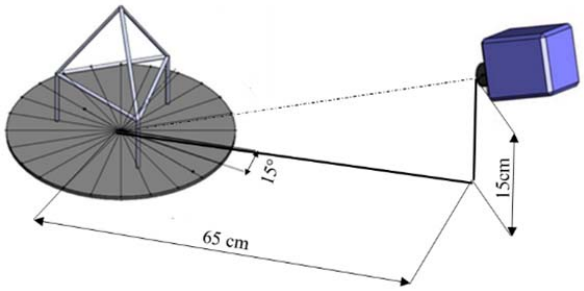

Fig. 6 The schematic of experimental setup

IV. Results and Discussion

The steps described in the methodology section were applied to the captured images to calculate ice loads on the structure. Fig. 7 (b) shows the result of tracing the structure in the image plane according to the camera position and the structure coordinates. In this case, the disk is located at the angle of 0°. Comparison between Figs. 7 (a) and (b) shows a good agreement between the image and the tracing of the structure. The ice area is detected using the Otsu thresholding method on this image by creating a binary image, Fig. 7 (c). Defining the structure coordinate, the joints between connected elements are removed to obtain the ice thickness of each element. The ice thicknesses of six structure elements are calculated independently, while overlaps appear in three elements. Ice thicknesses for elements with overlaps are estimated using this method.

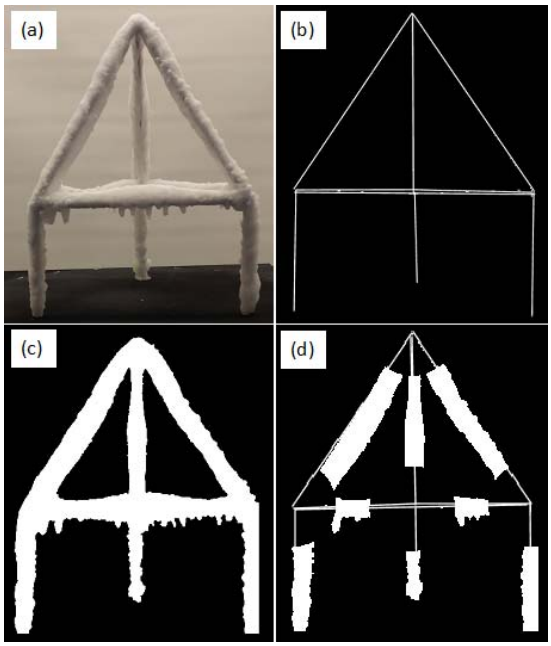

Fig. 7 Image processing results for the structure located at the angle of 0°; (a) Iced structure image, (b) locating structure scheme in the image plane, (c) Ice detection results, (d) Removing the joints using the structure scheme

Fig. 8 shows the results of image processing under the condition that the disk is rotated to 30°. In this case, the overlap involved four elements in the binary image, Fig. 8 (a). The algorithm calculates ice thicknesses for these four elements by subtracting the measured ice area and the area surrounded by elements. One of the elements appears short in the image; removing the corresponding joints in this case leads to eliminating ice detected on this element. The ice thickness of an element with similar properties is assigned as the thickness of this element.

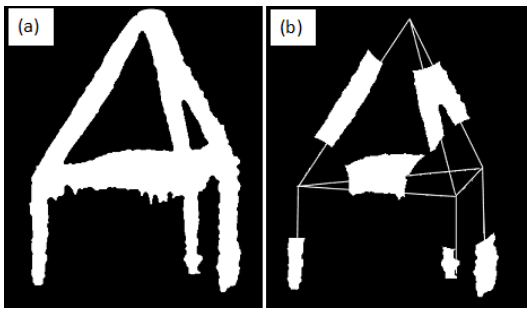

Fig. 8 Image processing results for the structure located at the angle of 30°; (a) Ice detection results, (b) Removing the joints using the structure scheme

Fig. 9 shows the ice detection and joint movement at the

angle of 165°. The ice thicknesses of four elements are calculated independently and ice thicknesses of other elements are estimated using the proposed method. At this angle, most structure elements are located in the camera view with a smaller ice diameter. As a result, underestimation of ice load calculation is expected.

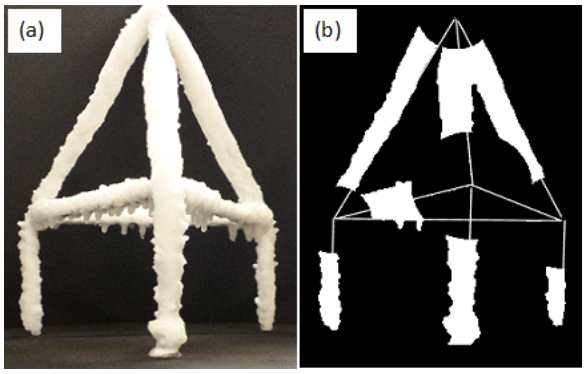

Fig. 9 Image processing results for the structure located at the angle of 165°; (a) Ice detection results, (b) Removing the joints using the structure scheme

Fig. 10 illustrates the numerical results of the ice load calculated in different 24 views and the actual ice load which is measured 700 g using a calibrated scale. Calculated ice loads fluctuate about the value of the actual ice load. Ice loads in different angles are mostly calculated with an error less than 20 percent. Overestimation and underestimation of the calculated ice load appear frequently. This fluctuation is the result of locating structure elements in different camera views, which is explained in the methodology section. For example, the majority of structure elements are presented in the image frame with their larger diameters at the location of 240°. At this location, the ice load is calculated 834 g, which is high overestimation at this angle. In another case, where the disk is located at 165°, the ice load is calculated approximately 550 g. This underestimation is due to appearing smaller diameters of the iced structure in the camera view. The average of ice load obtained at different angles is 670 g. This result shows a good agreement between the numerical results and the actual ice load. The average of calculated ice load is very close to the actual ice load value with an approximately 4 percent error.

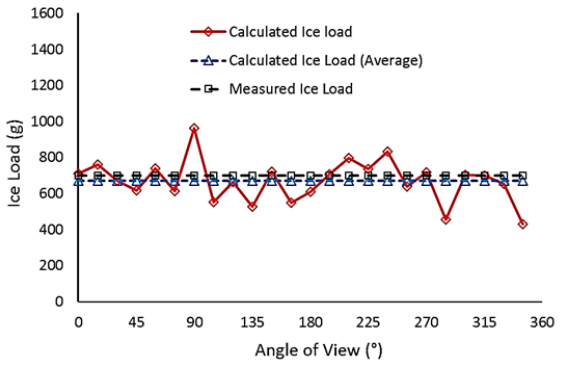

Fig. 10 Comparison between the calculated and measured ice loads

V. Conclusion

A numerical process is developed for ice detection and ice load measurement on a known structure applying an image processing method. A scheme of the structure is drawn in the image plane using the structure coordinates, camera position, and camera intrinsic and extrinsic parameters. The images of the iced structure are captured employing a camera located at the position used for tracing the structure schematic. The iced structure is detected in a binary image considering the Otsu thresholding method. As a result, the ice thickness of each component of ices structure is calculated. Overestimation and underestimation in ice thickness measurements occur due to the camera angle of view. The majority of the ice load measurements show a good agreement with the actual ice load value. However, in some cases, about 20 percent error occurs. Calculating the average of the ice loads neutralize the effect of over and underestimation, and the ice load is reported with less than 4 percent error.

Acknowledgment

The authors gratefully acknowledge the financial support from Statoil (Norway), MITACS, Petroleum Research Newfoundland and Labrador (PRNL) and ABS for this research.

References

[1] C. C. Ryerson, "Ice protection of offshore platforms," *Cold Reg. Sci. Technol.*, vol. 65, no. 1, pp. 97–110, 2011.
[2] A. Bodaghkhani, S.-R. Dehghani, Y. S. Muzychka, and B. Colbourne, "Understanding spray cloud formation by wave impact on marine objects," *Cold Reg. Sci. Technol.*, vol. 129, pp. 114–136, 2016.
[3] A. R. Dehghani-Sanij, S. R. Dehghani, G. F. Naterer, and Y. S. Muzychka, "Sea spray icing phenomena on marine vessels and offshore structures: review and formulation," *Ocean Eng.*, vol. 132, pp. 25–39, 2017.
[4] E. P. Lozowski, K. Szilder, and L. Makkonen, "Computer simulation of marine ice accretion," *Philos. Trans. R. Soc. London A Math. Phys. Eng. Sci.*, vol. 358, no. 1776, pp. 2811–2845, Nov. 2000.
[5] C. C. Ryerson, "Superstructure spray and ice accretion on a large U.S. Coast Guard cutter," *Atmos. Res.*, vol. 36, no. 3–4, pp. 321–337, 1995.
[6] C. C. Ryerson, "Assessment of Superstructure Ice Protection as Applied to Offshore Oil Operations Safety: Problems, Hazards, Needs, and Potential Transfer Technologies," *Erdc/Crrel Tr-08-14*, no. September, p. 156, 2008.
[7] D. J. Palmer A., "Development of a Marine Icing Monitoring System," *Proc. 20th Int. Conf. Port Ocean Eng. under Arct. Cond.*, pp. 1–12, 2009.
[8] X. Wang, J. Hu, B. Wu, L. Du, and C. Sun, "Study on edge extraction methods for image-based icing on-line monitoring on overhead transmission lines," *2008 Int. Conf. High Volt. Eng. Appl. ICHVE 2008*, pp. 661–665, 2008.
[9] C. Yu, Q. Peng, R. Wachal, and P. Wang, "An image-based 3D acquisition of ice accretions on power transmission lines," *Can. Conf. Electr. Comput. Eng.*, no. May, pp. 2005–2008, 2007.
[10] A. Fazelpour, S. R. Dehghani, V. Masek, and Y. S. Muzychka, "Effect of Ambient Conditions on Infrared Ice Thickness Measurement," in *IEEE Newfoundland Section Conference*, 2016.
[11] A. Fazelpour, S. R. Dehghani, V. Masek, and Y. S. Muzychka, "Infrared Image Analysis for Estimation of Ice Load on Structures," in *Arctic Technology Conference*, 2016.
[12] E. R. Davies, *Computer and Machine Vision: Theory*. 2012.
[13] N. Otsu, "A threshold selection method from gray-level histograms," *Automatica*, vol. 11, no. 285–296, pp. 23–27, 1975.
[14] R. C. S. Gonzalez and P. Wintz, "Digital image processing," 1977.